

## Experimental evidences for two paths in the dissolution process of B clusters in crystalline Si

D. De Salvador,<sup>a)</sup> E. Napolitani, G. Bisognin, and A. Carnera

MATIS-INFM (CNR) and Dipartimento di Fisica, Università di Padova, Via Marzolo 8, 35131 Padova, Italy

E. Bruno, S. Mirabella, G. Impellizzeri, and F. Priolo

MATIS-INFM (CNR) and Dipartimento di Fisica e Astronomia, Università di Catania, Via S. Sofia 64, 95123 Catania, Italy

(Received 13 June 2005; accepted 12 September 2005; published online 21 November 2005)

We show that B clusters, produced by self-interstitial interaction with substitutional B in crystalline Si, dissolve under annealing according to two distinct paths with very different characteristic times. The two regimes generally coexist, but while the faster dissolution path is predominant for clusters formed at low B concentration ( $1 \times 10^{19}$  B/cm<sup>3</sup>), the slower one is characteristic of clusters formed above the solubility limit and dominates the dissolution process at high B concentration ( $2 \times 10^{20}$  B/cm<sup>3</sup>). The activation energies of both processes are characterized and discussed. It is showed that the faster path can be connected to mobile B direct emission from small clusters, while the slower path is demonstrated not to be self-interstitial limited and it is probably related to a more complex cluster dissolution process. © 2005 American Institute of Physics.

[DOI: 10.1063/1.2126128]

Boron clustering is a widely studied phenomenon due to its relevance in micro- and nanoelectronics Si-based technology. At low concentration (below the solubility limit) B can cluster under the interaction with silicon self-interstitials (I) produced by ion implantation, forming clusters made of few atoms named boron interstitial clusters (BICs) that have been widely investigated experimentally and theoretically.<sup>1-8</sup> However, the increasing request for extremely highly doped shallow junctions imposes to implant B above the solubility limit (s.l.) for several applications. Relatively few works have investigated in detail this regime. In some papers the clustering that occurs at high B concentration is explained in terms of the same BIC model that explains low concentration clustering,<sup>9,10</sup> while in other cases the presence of a boride phase<sup>11</sup> or extended clusters containing boron<sup>12</sup> are reported.

In this letter we report a systematic investigation of the dissolution mechanisms of B clusters formed by Si ion implantation on samples with substitutional B at concentrations either above and below the s.l.. The kinetics of the B and I emission from the clusters is investigated in detail, and a coherent picture is given, based on the coexistence of two different classes of clusters, explaining both the concentration regimes.

We grew three 5 in. samples by molecular beam epitaxy (MBE), with a 15-nm-thick B box at different concentration levels placed at the depth of 215 nm, followed by four deeper B deltas (see Fig. 1) to monitor the I supersaturation.<sup>3-5</sup> During the MBE growth the base pressure was  $5 \times 10^{-11}$  mbar, the sample temperature was 460 °C and the Si growth rate 0.3 Å/s. This conditions allow us to grow fully substitutional B boxes as confirmed by measurements of strain by high resolution x-ray diffraction<sup>13</sup> and of substitutional fraction by nuclear reaction analysis channeling technique in thicker samples grown under the same condition. The cluster formation is induced by 20 keV,

$1 \times 10^{14}$  Si/cm<sup>2</sup> implant and subsequent annealing in N<sub>2</sub> atmosphere. We annealed the samples for 5 min at 815 °C in order to form the clusters and to completely recover the implant damage. The latter point has been checked by monitoring the transient enhanced diffusion of B of a reference sample without the B box, having only B deltas. The temperature of cluster formation (815 °C) and the B concentrations in the box have been chosen in order to have one sample below ( $1 \times 10^{19}$  B/cm<sup>3</sup>, sample 1), one just above ( $5 \times 10^{19}$  B/cm<sup>3</sup>, sample 2), and one five times above ( $2 \times 10^{20}$  B/cm<sup>3</sup>, sample 3) the s.l., which is of about  $4 \times 10^{19}$  B/cm<sup>3</sup> at 815 °C.<sup>14</sup>

In Fig. 1 we report the secondary ion mass spectrometry (SIMS) B concentration depth profiles of the high concentration B box (sample 3) together with the first two B deltas, before (dotted line) and after formation annealing (diamonds). A strong diffusion and an immobile peak in corre-

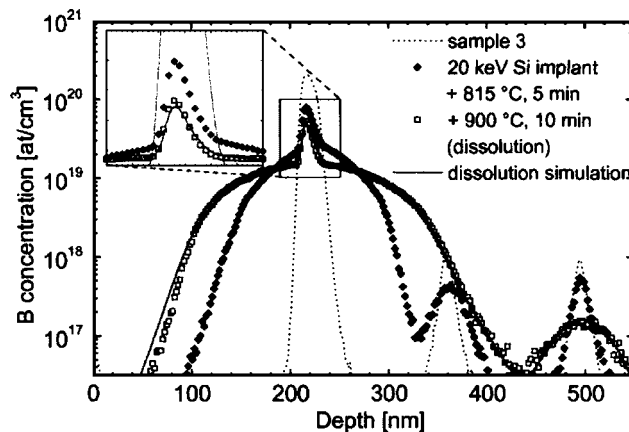


FIG. 1. SIMS boron concentration profile (dotted line) of the sample 3 (B box:  $2 \times 10^{20}$  B/cm<sup>3</sup>). Implantation and thermal annealing induce B clustering (diamonds). Further annealing at 900 °C induces B clusters dissolution (open squares), whose simulation is also displayed (continuous line). The inset is a magnification, on a linear vertical scale, of the squared region.

<sup>a)</sup>Electronic mail: desalvador@padova.infm.it

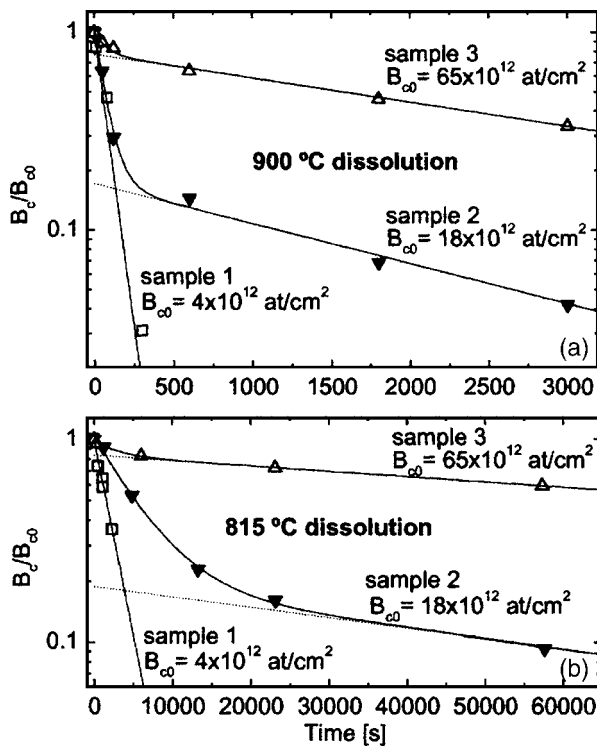


FIG. 2. Clustered B dose ( $B_c$ ) normalized to the clustered dose after formation ( $B_{c0}$ ) for sample 1 (B box:  $1 \times 10^{19}$  B/cm<sup>3</sup>, squares), sample 2 (B box:  $5 \times 10^{19}$  B/cm<sup>3</sup>, down triangles) and sample 3 (B box:  $2 \times 10^{20}$  B/cm<sup>3</sup>, up triangles) as a function of the dissolution time at temperature of 900 (a) or 815 °C (b). Continuous lines are a fit to the sum of two exponential decays, the slower of which is plotted with dotted lines.

spondence with the original box depth is clearly visible. Similar features are detected in the other two samples after the cluster formation process (not shown).

The formed clusters of the three samples are then dissolved at temperatures ranging from 815 to 1000 °C in inert ( $N_2$ ) atmosphere by rapid ramp thermal annealing up to 20 min and in conventional furnace for longer times. Figure 1 also shows the B profile of the sample 3 after the formation annealing and the dissolution at 900 °C for 10 min (open squares). A reduction of the clustered peak is clearly visible, together with a significant B diffusion both of the box and of the deltas. The clustered B profile at each annealing time, the average interstitial supersaturation between two subsequent annealing steps as well as the profile of the starting clustered B were obtained by a simultaneous fitting procedure of the B concentration profiles over the whole set of annealed samples.<sup>5</sup> The fitting model does not introduce any detailed hypothesis on the cluster structure and release mechanism. It is based on a rate equation system which only describes the dissolution of the clusters by considering as a fitting parameter the reduction rate of the immobile portion of the profile. The B concentration removed by the clustered profile increases the mobile portion of B profile which diffusion is described by I mediated diffusion equation including I supersaturation, extrinsic diffusion and field effects.<sup>5</sup> In Fig. 1 we reported the best fit of the diffused profiles obtained following this procedure. The quality of the fits in the figure is representative of the quality obtained over all the data.

In Fig. 2 the clustered B dose ( $B_c$ ) as extracted by the fitting procedure, normalized to the clustered B dose just after the formation process ( $B_{c0}$ ) is plotted as a function of

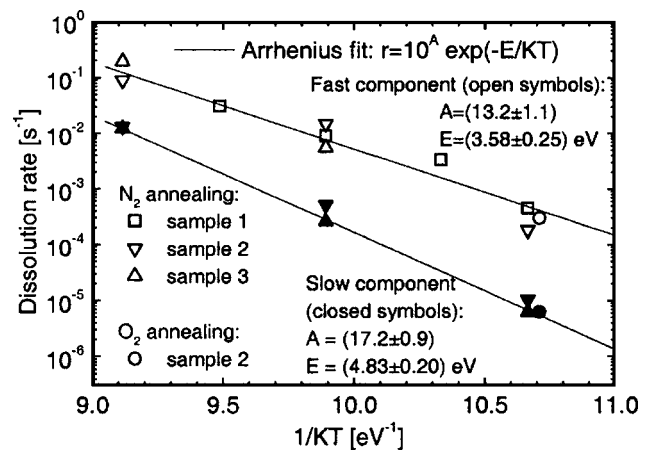


FIG. 3. Arrhenius plot of the dissolution rates of B clusters formed in sample 1, 2, and 3. Open (closed) symbols are relative to the faster (slower) process. All the processes were performed in  $N_2$  atmosphere, except for two processes (circles) performed in  $O_2$  atmosphere at 815 °C (slightly shifted towards lower temperatures, for clarity). Continuous lines are the best Arrhenius fits for the fast (upper line) and the slow (lower one) process obtained by a fit of all the data weighted by their errors (not shown).

annealing time at 900 °C [Fig. 2(a)] and 815 °C [Fig. 2(b)]. While the BIC dissolution in the sample 1 (squares) is well described by a single exponential decay, the sample 2 clearly presents two stages in the dissolution (down triangles). The first stage is quite fast and has a decay rate similar to that of previous one, while the second stage is much slower and involves a smaller fraction of  $B_{c0}$ . At higher B concentration (sample 3) two dissolution regimes are still visible. In this case, the fraction of the clustered B dissolving with the slower process is much higher, and the dissolution rate is very similar to the slowly dissolving clusters of the sample 2. The same trends, but with different characteristic times, are measured for the other dissolution temperatures not shown in Fig. 2. All the data were satisfactorily fitted supposing that the dissolution curve is the sum of two exponential decays with two different characteristic times (continuous lines in Fig. 2). We found that the weights of the two exponentials are independent of the dissolution temperature while they depend only on the starting sample. It is noteworthy that all the data are explained in terms of two distinct cluster populations dissolving with quite different characteristic times, a fast component and a slow component, which both are already present at the end of the formation process.

The slow component is totally absent in sample 1, whereas Fig. 2 shows that it is about the 20% and 80% of the whole starting clusters (intercept of dotted line) for samples 2 and 3, respectively. It is worth to note that the B concentration in excess with respect to the solubility limit is indeed exactly the 20% and the 80% of the total B concentration for sample 2 ( $5 \times 10^{19}$  B/cm<sup>3</sup>) and sample 3 ( $2 \times 10^{20}$  B/cm<sup>3</sup>), respectively. Therefore the slow dissolving component could be thought as arisen by the B atoms fraction above the B s.l., in both the samples.

More insights on the nature of the above clusters can be deduced by analyzing the dissolution kinetics as a function of the dissolution temperature. The dissolution rates obtained by the fitting of Fig. 2, together with those obtained at the other dissolution temperatures, are reported in Fig. 3. Open (closed) symbols are relative to the fast (slow) decay process. All the data, independently of the starting sample, can be

satisfactorily described by two Arrhenius fits (continuous lines) relative to the two components. Therefore, for the whole concentration range investigated, the dissolutions of the two components are two distinct thermally activated processes with two different exponential prefactors and activation energies the dissolution data of boron clusters reported in literature<sup>2,4,15</sup>. This suggests that the scattering of the literature data is probably due to the presence of these two main distinct processes in the cluster dissolution, never considered before. The faster process has an activation energy of  $3.58 \pm 0.25$  eV with a prefactor of  $10^{13.2 \pm 1.1} \text{ s}^{-1}$ , in agreement with our results of Ref. 5. The prefactor is compatible with that generally considered for a simple process of dissolution by direct emission of a mobile species related to the Si phonon frequency. The analysis of I supersaturation during the dissolution reveals a moderate supersaturation (10 at maximum) which decays with a rate similar to the fast component dissolution rate, while for longer times, where the slow component prevails, no supersaturation is detected. This indicates that the fast process is connected to a direct emission of both B and I, likeliest an emission of BI mobile complex. The earlier results, together with the fact that such clusters are formed even below the s.l., suggests that the fast dissolving component is directly connected to the usually considered small BICs. Our data demonstrate that such a kind of clusters is also present above the solubility limit coexisting with a different class of clusters.

As shown in Fig. 3, the slow dissolving component undergoes a dissolution process with a  $4.83 \pm 0.20$  eV activation energy and a prefactor of  $10^{17.2 \pm 0.9} \text{ s}^{-1}$ . This activation energy is in very good agreement with that determined in Ref. 9 (4.7 eV) by investigating B electrical reactivation after ultralow energy, high dose B implantation, with B concentrations well above the s.l. This suggests that the clusters of the slower component we observed are similar to the clusters responsible for B deactivation in ultra low energy B implants, which are relevant for ultrashallow junction formation.

The data of Mokhberi *et al.* were recently interpreted by theoretical simulations in Ref. 10 within the same model used to explain B–I clustering below the s.l. Within this framework, the long dissolution time is explained by the need for external interstitials, quite slowly supplied in equilibrium conditions, in order to dissolve such small, B rich clusters. In order to verify if our samples follow this interpretation, we performed a further experiment repeating the dissolution thermal processes at 815 °C in oxidizing O<sub>2</sub> atmosphere. In these conditions the I concentration exceeds about 10–20 times the equilibrium value<sup>16</sup> therefore any I limited process would have been accelerated by the same factor in O<sub>2</sub> atmosphere with respect to N<sub>2</sub> atmosphere. We performed the above experiment in sample 2, observing no difference at all between the dissolutions in O<sub>2</sub> and N<sub>2</sub> atmospheres (circles and down triangles in Fig. 3, respectively). This demonstrates that neither of the two cluster component dissolutions is I limited. Regarding the fast component, this result is in good agreement with the interpretation of a direct BI emission process given above. Regarding the slow com-

ponent, it excludes instead that the slow dissolving clusters formed at high B concentration can be interpreted as small, B rich BICs undergoing I-limited dissolution. Most likely we speculate that the slow dissolving component is constituted by larger clusters which dissolves with a more complicated dissolution mechanism similar to what proposed in Ref. 12. This idea is reinforced by considering that the prefactor of the slow dissolving process ( $10^{17.2 \pm 0.9} \text{ s}^{-1}$ ) is too high to be compatible with a simple direct emission dissolution path. It is instead similar to the prefactor determined for dissolution of larger defects, such as the {311} (about  $10^{16} \text{ s}^{-1}$ ).<sup>4</sup>

In conclusion, in the present work we report a clear evidence of the coexistence of two dissolution paths for boron clusters formed above B solubility limit under I supersaturation conditions. A faster dissolution path, related to small BICs dissolving through the direct emission of mobile species, is present for clustered B populations formed both above and below the solubility limit. A second, much slower dissolution path, is related to clusters formed with initial B concentration above the solubility limit. This last path cannot be explained on the basis of small clusters I-limited dissolution, whereas it is more likely related to a complex dissolution process involving clusters more extended than what is usually considered.

The authors wish to thank M. G. Grimaldi for nuclear reaction analysis, and R. Storti and A. Sambo for technical assistance. This work has been partially supported by the MIUR projects PRIN 2004 and FIRB.

<sup>1</sup>E. Michel, W. Rausch, P. A. Ronsheim, and R. H. Kasti, *Appl. Phys. Lett.* **50**, 416 (1987).

<sup>2</sup>L. Pelaz, G. H. Gilmer, H.-J. Gossmann, C. S. Rafferty, M. Jaraiz, and J. Barbolla, *Appl. Phys. Lett.* **74**, 3657 (1999), and references therein.

<sup>3</sup>G. Mannino, N. E. B. Cowern, F. Roozeboom, and J. G. M. van Berkum, *Appl. Phys. Lett.* **76**, 855 (2000).

<sup>4</sup>S. C. Jain, W. Schoenmaker, R. Lindsay, P. A. Stolk, S. Decoutere, M. Willander, and H. E. Maes, *J. Appl. Phys.* **91**, 8919 (2002), and references therein.

<sup>5</sup>S. Mirabella, E. Bruno, F. Priolo, D. De Salvador, E. Napolitani, A. V. Drigo, and A. Carnera, *Appl. Phys. Lett.* **83**, 680 (2003).

<sup>6</sup>X. Liu, W. Windl, and M. Masquelier, *Appl. Phys. Lett.* **77**, 2018 (2000).

<sup>7</sup>T. J. Lenosky, B. Sadigh, S. K. Theiss, M. J. Caturla, and T. D. de la Rubia, *Appl. Phys. Lett.* **77**, 1834 (2000).

<sup>8</sup>P. Alippi, P. Ruggerone, and L. Colombo, *Phys. Rev. B* **69**, 125205 (2004); M. Cogoni, A. Mattoni, B. P. Uberuaga, A. F. Voter, and L. Colombo, *Appl. Phys. Lett.* (2005) (in press).

<sup>9</sup>A. Mokhberi, P. B. Griffin, J. D. Plummer, E. Paton, S. McCoy, and K. Elliot, *IEEE Trans. Electron Devices* **49**, 1183 (2002).

<sup>10</sup>M. Aboy, L. Pelaz, L. A. Marques, P. Lopez, J. Barbolla, and R. Duffy, *J. Appl. Phys.* **97**, 103520 (2005).

<sup>11</sup>A. Agarwal, H.-J. Gossmann, and D. J. Eaglesham, *Appl. Phys. Lett.* **74**, 2331 (1999).

<sup>12</sup>F. Cristiano, X. Hebras, N. Cherkashin, A. Claverie, W. Lerch, and S. Paul, *Appl. Phys. Lett.* **83**, 5407 (2003).

<sup>13</sup>G. Bisognin, D. De Salvador, E. Napolitani, A. Carnera, E. Bruno, S. Mirabella, and F. Priolo (unpublished).

<sup>14</sup>A. Armigliato, D. Nobili, P. Ostojka, M. Servidori, S. Solmi, in *Electrochem. Soc. Proc. 77-2: Semiconductor Silicon 1977*, edited by H. R. Huff and E. Sirtl, 1977, p. 638.

<sup>15</sup>M. Uematsu, *J. Appl. Phys.* **84**, 4781 (1998).

<sup>16</sup>E. Napolitani, M. Di Marino, D. De Salvador, A. Carnera, M. Spadafora, S. Mirabella, and A. Terrasi, S. Scalese, *J. Appl. Phys.* **97**, 036106 (2005).